

# Conjugated Donor–Acceptor Copolymer Semiconductors with Large Intramolecular Charge Transfer: Synthesis, Optical Properties, Electrochemistry, and Field Effect Carrier Mobility of Thienopyrazine-Based Copolymers

Yan Zhu, Richard D. Champion, and Samson A. Jenekhe\*

Department of Chemical Engineering and Department of Chemistry, University of Washington, Seattle, Washington 98195-1750

Received August 13, 2006; Revised Manuscript Received September 27, 2006

**ABSTRACT:** Several conjugated thieno[3,4-*b*]pyrazine-based donor–acceptor copolymers were synthesized by Stille and Suzuki copolymerizations, and their optical, electrochemical, and field-effect charge transport properties were characterized. The new copolymers, poly(5,7-bis(3-dodecylthiophen-2-yl)thieno[3,4-*b*]pyrazine) (BTTP), poly(5,7-bis(3-dodecylthiophen-2-yl)thieno[3,4-*b*]pyrazine-*alt*-2,5-thiophene) (BTTP-T), poly(5,7-bis(3-dodecylthiophen-2-yl)thieno[3,4-*b*]pyrazine-*alt*-9,9-dioctyl-2,7-fluorene) (BTTP-F), and poly(5,7-bis(3-dodecylthiophen-2-yl)thieno[3,4-*b*]pyrazine-*alt*-1,4-bis(decyloxy)phenylene) (BTTP-P), had moderate to high molecular weights, broad optical absorption bands that extend into the near-infrared region with absorption maxima at 667–810 nm, and small optical band gaps (1.1–1.6 eV). They showed ambipolar redox properties with low ionization potentials (HOMO levels) of 4.6–5.04 eV. The field-effect mobility of holes varied from  $4.2 \times 10^{-4} \text{ cm}^2/(\text{V s})$  in BTTP-T to  $1.6 \times 10^{-3} \text{ cm}^2/(\text{V s})$  in BTTP-F. These results show that thieno[3,4-*b*]pyrazine-based donor–acceptor copolymers combine small optical band gaps with fairly high carrier mobilities and thus are promising for organic electronic devices.

## Introduction

Conjugated polymer semiconductors with electron donor–acceptor architectures are of growing interest for organic electronic applications,<sup>1–5</sup> including photovoltaic cells,<sup>3</sup> light-emitting diodes (LEDs),<sup>4</sup> and field-effect transistors (FETs).<sup>5</sup> Intramolecular charge transfer (ICT) interaction between the electron donor (D) and electron acceptor (A) units within D–A copolymers can facilitate ready manipulation of their electronic structures (HOMO/LUMO levels) and thus electronic and optoelectronic properties.<sup>1–5</sup> Through the careful design and selection of the donor (p-type) and acceptor (n-type) building blocks, the strength of ICT can be tuned, allowing such D–A copolymer semiconductors to exhibit small band gaps, broad absorption bands that extend into the near-infrared spectral range, high electron affinity and low ionization potential,<sup>3–5</sup> efficient photoinduced charge transfer and separation,<sup>3</sup> and ambipolar charge transport with high mobilities.<sup>5b,c</sup> Conjugated donor–acceptor copolymers with strong intramolecular charge transfer between the donor and acceptor moieties are of special interest for photovoltaic applications because their small band gaps, broad absorption spectra, and ambipolar charge transport could facilitate efficient harvesting of the solar spectrum and improve charge photogeneration and collection.<sup>3</sup>

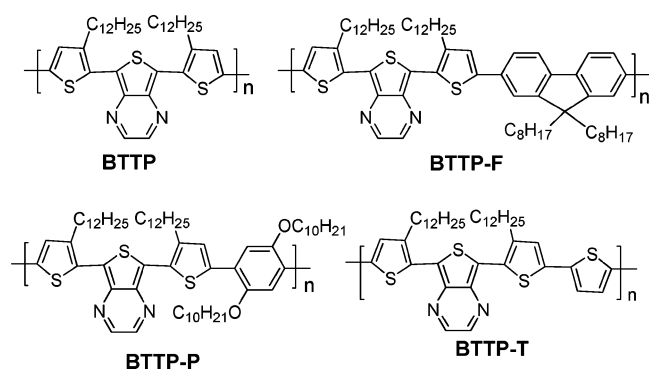
Although many electron-accepting moieties, including quinoxaline,<sup>2</sup> quinoxaline,<sup>2d,4b,5a</sup> 2,1,3-benzothiadiazole,<sup>3g</sup> and pyridazine,<sup>5f</sup> have been explored in  $\pi$ -conjugated D–A copolymer systems, their electron-accepting properties, and thus the strength of the ICT in most of these copolymers, are not strong enough to extend the absorption bands into the near-infrared. A few strong electron acceptors, such as thieno[3,4-*b*]pyrazine,<sup>3e,f,4d</sup> [1,2,5]-thiadiazolo[3,4-*g*]quinoxaline,<sup>5e</sup> and pyrazino[2,3-*g*]quinoxaline,<sup>2e</sup> have been incorporated into donor–acceptor conjugated poly-

mers to achieve small band gap polymer semiconductors for electronic device applications. Although the charge carrier transport properties of conjugated D–A copolymers are critical to their applications in photovoltaic cells, LEDs, and thin film transistors, only a few of these materials have known carrier mobility.<sup>5</sup> The hole mobility and ambipolar charge carrier transport in thiophene–quinoxaline and thiophene–thiadiazole copolymers were recently reported by our group<sup>5a</sup> and others.<sup>5c</sup> A [1,2,5]thiadiazolo[3,4-*g*]quinoxaline-based D–A oligomer was also recently showed to have a field-effect hole mobility as high as  $0.03 \text{ cm}^2/(\text{V s})$ .<sup>5c</sup> This latter result suggests that higher hole mobility may be achievable with high molecular weight D–A copolymers since the charge carrier mobility of conjugated polymers strongly depends on molecular weight.<sup>6</sup>

In this paper, we report the synthesis, electrochemical and optical properties, and field-effect carrier mobility of a series of new conjugated donor–acceptor copolymer semiconductors based on thieno[3,4-*b*]pyrazine as the electron acceptor comonomer. Four new conjugated copolymers were synthesized by Stille or Suzuki polymerization and investigated, including poly(5,7-bis(3-dodecylthiophen-2-yl)thieno[3,4-*b*]pyrazine) (BTTP), poly(5,7-bis(3-dodecylthiophen-2-yl)thieno[3,4-*b*]pyrazine-*alt*-2,5-thiophene) (BTTP-T), poly(5,7-bis(3-dodecylthiophen-2-yl)thieno[3,4-*b*]pyrazine-*alt*-9,9-dioctyl-2,7-fluorene) (BTTP-F), and poly(5,7-bis(3-dodecylthiophen-2-yl)thieno[3,4-*b*]pyrazine-*alt*-1,4-bis(decyloxy)phenylene) (BTTP-P) (Chart 1). The parent conjugated copolymer BTTP (Chart 1) has an alternating acceptor (A)–donor (D) chain structure of the form  $\cdots\text{A} - \text{DD} - \text{A} - \text{DD} \cdots$ , where A is thieno[3,4-*b*]pyrazine and D is 2,5-linked thiophene. To allow for the systematic modulation of the ICT strength and thus the electronic and optical properties, derivatives with a chain structure  $\cdots\text{A} - \text{DED} - \text{A} - \text{DED} \cdots$  were designed, where the moiety E is a dialkylfluorene, dialkoxyphenylene, or thiophene. We show that these D–A copolymers exhibiting strong intramolecular charge transfer have

\* Author for all correspondence. E-mail: jenekhe@u.washington.edu.

Chart 1



very small optical band gaps (1.1–1.6 eV), broad absorption bands that extend into the near-IR region, and ambipolar redox properties with rather small ionization potentials (4.6–5.04 eV). Initial organic field-effect transistors (OFETs) made from the copolymer semiconductors showed field effect hole mobilities of up to  $1.6 \times 10^{-3} \text{ cm}^2/(\text{V s})$ . We note that while our work was in progress a report of an octyl derivative of BTTP synthesized by oxidative  $\text{FeCl}_3$  polymerization appeared.<sup>3f</sup>

## Results and Discussion

**Synthesis and Characterization.** The synthetic routes to the monomers and polymers are outlined in Scheme 1. The coupling reaction between the Grignard reagent of 2-bromo-3-dodecylthiophene and 5,7-dibromothieno[3,4-*b*]pyrazine in the presence of a catalytic amount of  $\text{NiCl}_2(\text{dppp})$  afforded compound **1**. Bromination of **1** by *N*-bromosuccinimide (NBS) gave the dibromo monomer **2**. The monomer **3**, 2,5-didecyloxyphenylene-1,4-bis(4,4,5,5-tetramethyl-1,3,2-dioxaborolane), was prepared by the boronation of 1,4-dibromo-2,5-bis(decyloxy)benzene with 2-isopropoxy-4,4,5,5-tetramethyl-1,3,2-dioxaborolane. Poly(5,7-bis(3-dodecylthiophen-2-yl)thieno[3,4-*b*]pyrazine) (BTTP) and poly(5,7-bis(3-dodecylthiophen-2-yl)thieno[3,4-*b*]pyrazine-*alt*-2,5-thiophene) (BTTP-T) were synthesized by Pd(0)-mediated Stille coupling polymerization in chlorobenzene. Poly(5,7-bis(3-dodecylthiophen-2-yl)thieno[3,4-*b*]pyrazine-*alt*-9,9-dioctyl-2,7-fluorene) (BTTP-F) and poly(5,7-bis(3-dodecylthiophen-2-yl)thieno[3,4-*b*]pyrazine-*alt*-1,4-bis(decyloxy)phenylene) (BTTP-P) were synthesized by Suzuki coupling polymerization in high yields (90–95%). All the copolymers except BTTP-T were partly soluble in organic solvents such as chloroform, toluene, and chlorobenzene at room temperature and completely soluble in high boiling point solvents (e.g., chlorobenzene) at high temperature. BTTP-T was not soluble in most organic solvents probably due to its high molecular weight or the absence of solubilizing groups on the extra thiophene ring. The weight-average molecular weights ( $M_w$ ) of BTTP, BTTP-F, and BTTP-P were determined by gel permeation chromatography (GPC) against polystyrene standards in trichlorobenzene and found to be 5300–172 600 with a polydispersity index ( $M_w/M_n$ ) of 1.51–3.69 (Table 1). The molecular weight of BTTP-T was not determined by GPC because of its poor solubility in organic solvents. We note that the molecular weight of BTTP is a factor of 2 higher compared to a similar 3-octylthiophene-thieno[3,4-*b*]pyrazine copolymer that was made by oxidative polymerization with ferric chloride.<sup>3f</sup> Although the molecular weight of BTTP is not high, it can be increased by optimizing the Stille polymerization condition, such as use of different solvents or catalysts.

The molecular structures of the copolymers were verified by  $^1\text{H}$  NMR, FT-IR, and UV-vis spectra. The  $^1\text{H}$  NMR spectra

of the copolymers were in good agreement with their structures. The  $^1\text{H}$  NMR spectra of BTTP, BTTP-F, and BTTP-P are shown in Figure 1. The singlet resonance at 8.61 ppm, assigned to the two protons (labeled “a” in Figure 1) adjacent to the imine nitrogen atoms of thienopyrazine unit, was observed in the spectra of all the copolymers. The resonances at 7.24, 7.39, and 7.35 ppm in the spectra of BTTP, BTTP-F, and BTTP-P, respectively, are assigned to the two protons in the thiophene ring. Resonances at 7.66–7.73 ppm in the spectrum of BTTP-F are assigned to the protons in the fluorene ring. The peak at 7.61 ppm in the BTTP-P spectrum corresponds to the two protons in the phenylene ring. The peaks in the range 0.9–4.19 ppm arise from alkyl groups in the copolymers; the peak area ratio between the aromatic and aliphatic protons in the NMR spectra agrees with the molecular structures of the copolymers. FT-IR spectra of the copolymers also confirmed their molecular structures. The vibrational bands at  $1535 \text{ cm}^{-1}$  in all the copolymers are due to stretching vibrations of the  $\text{C}=\text{N}$  group and are characteristic of the thieno[3,4-*b*]pyrazine ring. The strong bands at about  $1468 \text{ cm}^{-1}$  are assigned to the stretching vibrations of  $\alpha,\alpha'$ -coupled thiophene rings.

The thermogravimetric analysis (TGA) scans of the four copolymers are shown in Figure 2. The TGA thermograms revealed that the onset decomposition temperatures of the D–A copolymers under nitrogen were in the range 378–410 °C (Table 1), indicative of good thermal stability. BTTP has a 5% weight loss before its onset decomposition temperature at 378 °C probably because of the low molecular weight portion in this copolymer. The thermal transitions of the copolymers were investigated by differential scanning calorimetry (DSC). Copolymers BTTP-P and BTTP-T exhibited broad endotherms centered at 250 and 310 °C, respectively, in the second-heating DSC scans. BTTP showed a crystallization peak at 175 °C and no melting peaks up to 350 °C. BTTP-F showed a glass transition temperature of 97 °C and no crystallization and melting transitions up to 350 °C.

**Optical Properties.** The optical absorption spectra of the model compound, 5,7-bis(3-dodecylthiophen-2-yl)thieno[3,4-*b*]pyrazine (**1**), in dilute ( $10^{-6} \text{ M}$ ) toluene solution, the copolymers in dilute ( $10^{-6} \text{ M}$ ) chlorobenzene solution, and the thin films of soluble copolymers (BTTP, BTTP-P, and BTTP-F) are shown in Figure 3. The dilute chlorobenzene solution of BTTP-T was filtered by using a  $0.45 \mu\text{m}$  filter to remove insoluble residue before the absorption spectrum was obtained. The optical absorption spectrum of BTTP-T thin film was not recorded due to its poor solubility in most organic solvents. The main optical properties of the D–A copolymers are collected in Table 2. The 305 nm band in the absorption spectrum of the model compound **1** in dilute solution can be assigned to the  $\pi$ – $\pi^*$  transition whereas the 506 nm band is due to intramolecular charge transfer (ICT)<sup>1</sup> between the thiophene donor and the thieno[3,4-*b*]pyrazine acceptor moieties. Similarly, the absorption spectra of the copolymers in dilute solutions are characterized by two bands, one near 417–425 nm and the other centered at 612–745 nm (Figure 3A). The former band can be assigned to  $\pi$ – $\pi^*$  transition whereas the lowest energy band is due to ICT between the donor and the thieno[3,4-*b*]pyrazine acceptor moieties. The solution absorption spectrum of BTTP-T, with an absorption maximum ( $\lambda_{\text{max}}^{\text{abs}}$ ) at 745 nm (1.66 eV), is broadened and red-shifted compared to those of BTTP ( $\lambda_{\text{max}}^{\text{abs}} = 675 \text{ nm}$ ), BTTP-P ( $\lambda_{\text{max}}^{\text{abs}} = 630 \text{ nm}$ ), and BTTP-F ( $\lambda_{\text{max}}^{\text{abs}} = 612 \text{ nm}$ ). This can be explained by the much stronger ICT effects in the BTTP-T copolymer than those in BTTP, BTTP-P, and BTTP-F. Among these four copolymers, BTTP-T has an

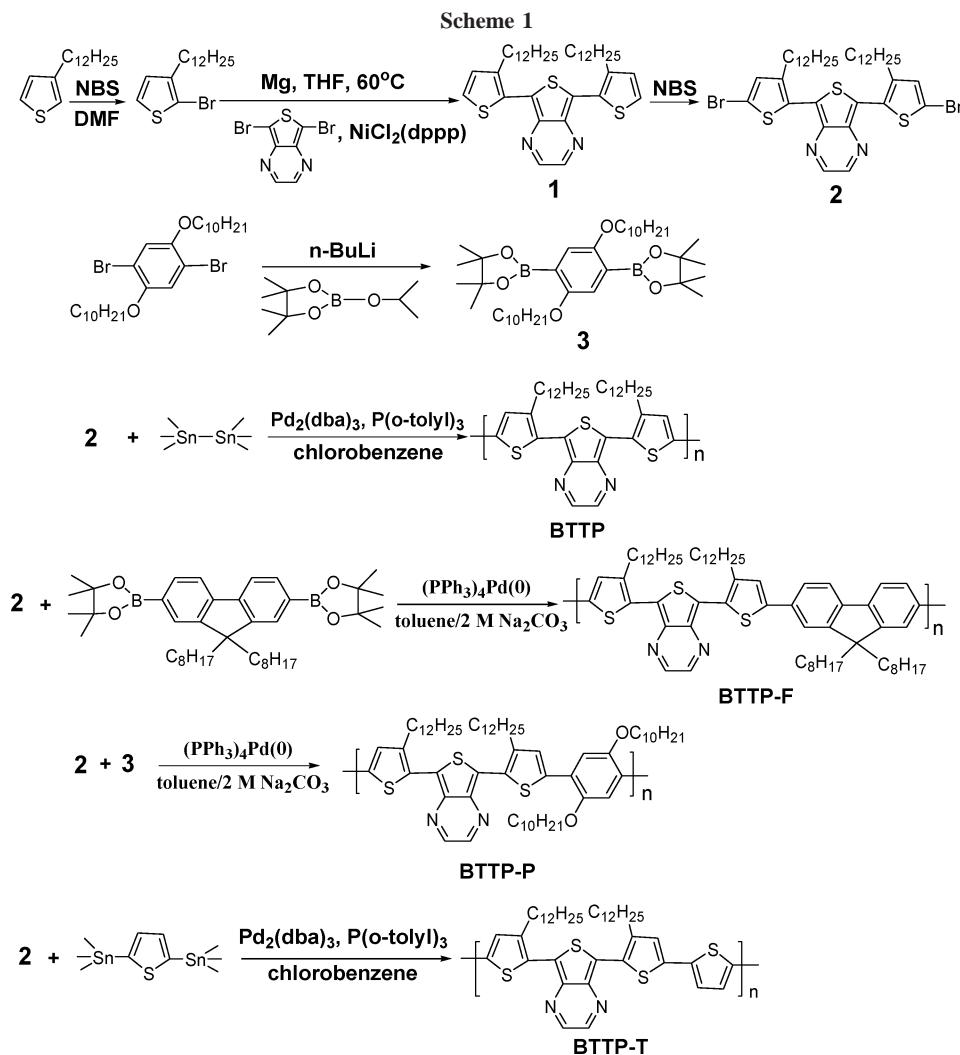


**Table 1. Molecular Weights,<sup>a</sup> Thermal Properties, and Hole Mobility of Copolymers**

polymer	yield (%)	$M_w$	$M_w/M_n$	$T_d^c$ (°C)	$\mu_h$ (cm <sup>2</sup> /(V s))
BTTP	53	5300	1.51	378	$7.1 \times 10^{-4}$
BTTP-F	94	172600	3.69	410	$1.6 \times 10^{-3}$
BTTP-P	90	10000	1.59	397	$1.1 \times 10^{-3}$
BTTP-T	95	— <sup>b</sup>	— <sup>b</sup>	405	$4.2 \times 10^{-4}$

<sup>a</sup> Molecular weights determined by GPC in trichlorobenzene at 135 °C using polystyrene standards. <sup>b</sup> Not determined due to the poor solubility in organic solvents. <sup>c</sup> Onset decomposition temperature measured by TGA under N<sub>2</sub>.

alternating  $\cdots A-DDD-A-DDD\cdots$  chain structure and high degree of electronic delocalization. In the chain structures of BTTP-P and BTTP-F,  $\cdots A-DED-A-DED\cdots$ , the additional dialkoxylphenylene or dialkylfluorene moiety (E) is a poorer electron-donating unit compared to thiophene, and it significantly lowers the chain structure symmetry, resulting in a large decrease in the ICT and thus electronic delocalization.

Figure 3B shows the optical absorption spectra of thin films of the thieno[3,4-*b*]pyrazine-based copolymers. The thin film absorption spectra are generally similar in shape to those in dilute solutions with two characteristic bands centered at 442–474 and 667–810 nm. The absorption maximum of BTTP-F at 667 nm is 55 nm red-shifted compared to the corresponding spectrum in dilute solution. In the case of BTTP-P and BTTP, their absorption spectra in the solid state exhibit huge red shifts (180 nm for BTTP-P and 105 nm for BTTP) in the lowest-energy absorption maxima compared to the corresponding

spectra in dilute solutions. The large increase in the electronic delocalization length of the copolymers in the solid state is explained by their much more planar conformations in the solid state. Both BTTP-P and BTTP have very broad absorption bands that extend into the near-infrared region with a  $\lambda_{\max}$  at 810 nm for BTTP-P and 780 nm for BTTP. The optical band gap ( $E_g^{\text{opt}}$ ) derived from the absorption edge of the thin film spectra was in the range 1.1–1.6 eV (Table 2). As expected, BTTP with the strongest intramolecular charge-transfer interaction has the smallest optical band gap, 1.1 eV, which is much smaller than that of poly(3-alkylthiophene) homopolymer ( $\sim 2.0$  eV).<sup>7</sup> This further supports the idea that the ICT interaction between donor and acceptor moieties in D–A copolymers is an efficient method to lower the band gap of conjugated polymers.<sup>1,3e–h</sup> The 1.1 eV band gap of BTTP is comparable to that of a similar 3-octylthiophene–thieno[3,4-*b*]pyrazine copolymer (1.3 eV).<sup>3f</sup> However, we note that the optical band gaps of electrochemically synthesized poly(2,3-dialkylthieno[3,4-*b*]pyrazine) homopolymers have been reported to be as small as 0.66–0.79 eV,<sup>8</sup> which is very unusual when compared to the present donor–acceptor conjugated copolymers.<sup>1,3e–h</sup> The small optical band gaps and very broad absorption bands of these thieno[3,4-*b*]pyrazine-based copolymer semiconductors suggest that they could be useful materials for photovoltaic applications.<sup>3</sup>

The normalized photoluminescence (PL) emission spectra of the model compound **1** and some of the thieno[3,4-*b*]pyrazine-based D–A copolymers are shown in Figure 4. The PL spectrum of BTTP-T was not recorded due to its poor solubility in organic

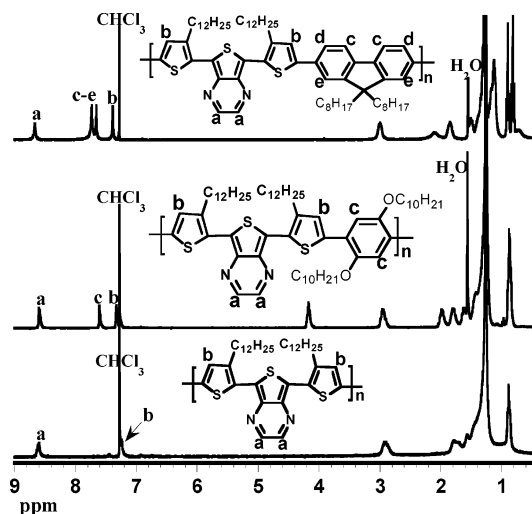


**Figure 1.**  $^1\text{H}$  NMR spectra of copolymers in  $\text{CDCl}_3$  and their assignment.

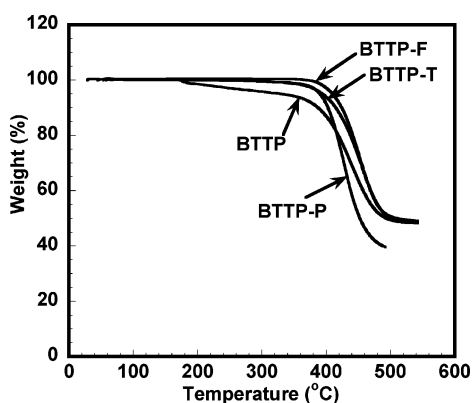


**Figure 2.** TGA thermograms of thieno[3,4-*b*]pyrazine-based donor-acceptor copolymers in  $\text{N}_2$ .

solvents. Compound **1** shows red PL emission with  $\lambda_{\text{max}}^{\text{em}} = 652$  nm in dilute toluene solution. BTTP-F has a broad, featureless emission band centered at 760 nm in chlorobenzene solution and at 785 nm in thin film. Although the broad and featureless emission bands of conjugated thin films are commonly due to aggregation and excimer emission,<sup>9</sup> the weak PL emission of the present donor-acceptor copolymers originates from ICT excited states. BTTP and BTTP-P similarly had broad emission bands with peaks at 734 nm (BTTP) and 798 nm (BTTP-P) in dilute chlorobenzene solutions. Both BTTP and BTTP-P have no detectable emission in thin films.

**Electrochemical Properties.** The electronic states, ionization potential/electron affinity (HOMO/LUMO levels), of the soluble thieno[3,4-*b*]pyrazine-based conjugated donor-acceptor copolymers were investigated by cyclic voltammetry (CV). The oxidation and reduction cyclic voltammograms of the copolymer thin films are shown in Figure 5, and all the electrochemical data are summarized in Table 2. The copolymers have reversible oxidation and reversible reduction as evident from the areas and close proximity of the anodic and cathodic peaks. The formal reduction potentials of BTTP, BTTP-P, and BTTP-F are  $-1.4$ ,  $-1.73$ , and  $-1.9$  V (vs SCE), respectively. The formal oxidation potentials of the copolymers are in the range  $0.29$ – $0.71$  V (vs SCE).

The onset oxidation potential and onset reduction potential of the parent copolymer BTTP are  $0.2$  and  $-1.3$  V, respectively, from which we estimate an ionization potential (IP, HOMO level) of  $4.6$  eV ( $\text{IP} = E_{\text{ox}}^{\text{onset}} + 4.4$ )<sup>10</sup> and an electron affinity

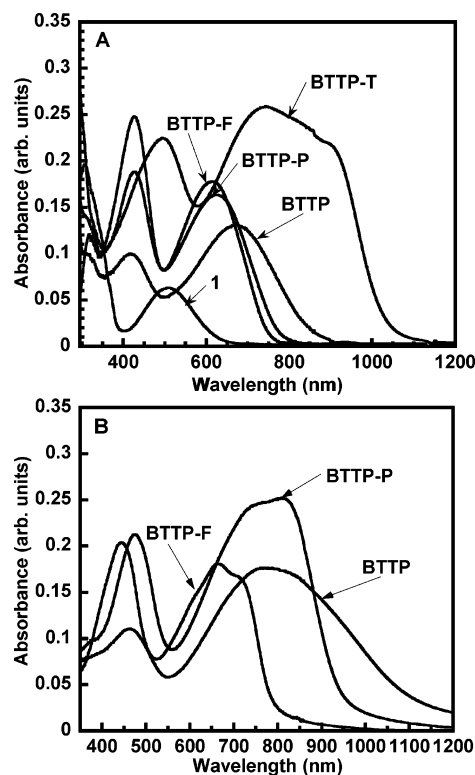


**Figure 3.** Optical absorption spectra of compound **1** in a  $10^{-6}$  M toluene solution and D-A copolymers in  $10^{-6}$  M chlorobenzene solutions (A) and as thin films on glass substrates (B).

(EA, LUMO level) of  $3.1$  eV ( $\text{EA} = E_{\text{red}}^{\text{onset}} + 4.4$ ).<sup>10</sup> The  $4.6$  eV IP value of BTTP is  $0.3$  eV less than that of poly(3-hexylthiophene) ( $4.9$  eV), whereas its EA value ( $3.1$  eV) is  $0.6$  eV higher than that reported for the poly(2,3-dioctylthieno[3,4-*b*]pyrazine) homopolymer ( $\sim 2.5$  eV).<sup>8</sup> The lower IP and higher EA values of BTTP compared to those of the homopolymers poly(A) and poly(D) are clearly due to the strong intramolecular charge transfer exhibited by this D-A copolymer. Similar reversible oxidation and reversible reduction were observed in an electropolymerized thieno[3,4-*b*]pyrazine-thiophene copolymer.<sup>3f</sup> The IP and EA values of BTTP-F were similarly estimated to be  $5.04$  and  $2.8$  eV, respectively. Given that the HOMO and LUMO levels of poly(9,9-octylfluorene) (PFO) are  $5.6$  and  $2.0$  eV, respectively, when measured under the same conditions, it is clear that the HOMO/LUMO levels of BTTP-F have been significantly varied relative to those of PFO and BTTP due to the modulated ICT strength. Our IP value for BTTP-F is almost identical to that reported for a similar copolymer of fluorene, thiophene, and thieno[3,4-*b*]pyrazine (APFO-Green 2), whereas the EA value of BTTP-F is  $0.7$  eV less than that of APFO-Green 2.<sup>3h</sup> An IP value of  $4.64$  eV and EA value of  $2.8$  eV were found in the case of BTTP-P. The highly reversible electrochemical oxidation and reduction and low IP values of these D-A copolymers suggest good prospects for efficient hole/electron injection/transport in organic electronic devices. The electrochemical band gap ( $E_{\text{g}}^{\text{el}} = \text{IP} - \text{EA}$ ) was determined to be  $1.5$  eV for BTTP,  $1.84$  eV for BTTP-P, and  $2.24$  eV for BTTP-F, which are  $0.4$ – $0.6$  eV larger than the optically determined ones ( $E_{\text{g}}^{\text{opt}} = 1.1$ – $1.6$  eV). This difference can be explained by the exciton binding energy of conjugated polymers which is thought to be in the range of  $\sim 0.4$ – $1.0$  eV.<sup>11</sup>

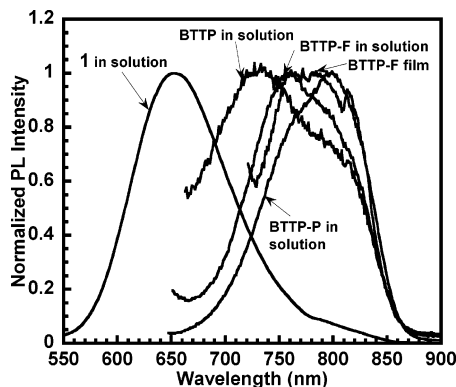
**Field-Effect Transistor Characteristics.** The field-effect carrier mobilities of the thieno[3,4-*b*]pyrazine-based D-A copolymers were investigated by fabricating and evaluating thin film field-effect transistors based on the bottom contact geometry



Table 2. Optical and Redox Properties of Copolymers

copolymer	$\lambda_{\text{max}}^{\text{abs}}$ (nm)		$E_{\text{g}}^{\text{opt}}$ (eV)	$E_{\text{ox}}^{\text{onset}}$ (V)	$E_{\text{ox}}^{\text{o}}$ (V)	IP <sup>c</sup> (eV)	$E_{\text{red}}^{\text{onset}}$ (V)	$E_{\text{red}}^{\text{o}}$ (V)	EA <sup>d</sup> (eV)	$E_{\text{g}}^{\text{cl}}$ (eV)
	solution	film								
BTTP	675	780	1.1	0.2	0.5	4.6	−1.3	−1.4	3.1	1.5
BTTP-P	630	810	1.3	0.24	0.29	4.64	−1.6	−1.73	2.8	1.84
BTTP-F	612	667	1.6	0.67	0.71	5.04	−1.64	−1.9	2.8	2.24

<sup>a</sup> Onset oxidation and reduction potentials vs SCE. <sup>b</sup> Formal oxidation and reduction potentials vs SCE. <sup>c</sup> Ionization potential was obtained based on  $\text{IP} = E_{\text{ox}}^{\text{onset}} + 4.4$  eV. <sup>d</sup> Electron affinity was obtained based on  $\text{EA} = E_{\text{red}}^{\text{onset}} + 4.4$  eV.



**Figure 4.** PL emission spectra of compound **1** in  $10^{-6}$  M toluene solution, D–A copolymers in  $10^{-6}$  M chlorobenzene solutions, and a thin BTTP-F film on a glass substrate.

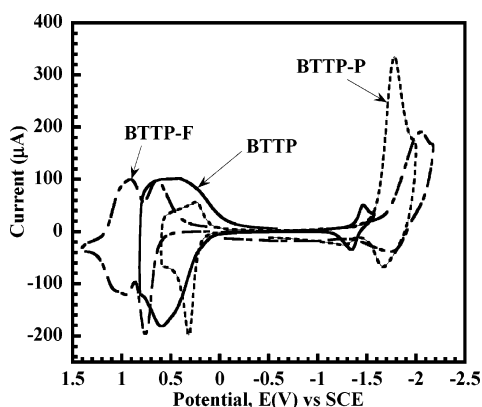


**Figure 5.** Cyclic voltammograms of D–A copolymer thin films in 0.1 M  $\text{Bu}_4\text{NPF}_6$  solution in acetonitrile at a scan rate of 40 mV/s.

similar to our previous reports.<sup>12a–c</sup> The copolymers showed typical p-channel output characteristics (plot of drain current  $I_D$  vs drain voltage  $V_D$  at different gate voltages  $V_G$ ) when operated in the accumulation mode.<sup>13</sup> In the saturation region,  $I_D$  can be described by eq 1:<sup>13</sup>

$$I_D = (W/2L)C_0\mu_h(V_G - V_T)^2 \quad (1)$$

where  $\mu_h$  is the field-effect hole mobility,  $W$  is the channel width,  $L$  is the channel length,  $C_0$  is the capacitance per unit area of the gate dielectric layer ( $\text{SiO}_2$ , 300 nm,  $C_0 = 11$  nF/cm<sup>2</sup>), and  $V_T$  is the threshold voltage. The saturation region field-effect mobility was thus calculated from the transfer characteristics of the OFETs involving plotting  $I_D^{1/2}$  vs  $V_G$ . To promote the molecular chain ordering of the polymer semiconductor at the gate dielectric/semiconductor interface, the gate dielectric surface was modified by the silylating agent octadecyltrichlorosilane (OTS-18).<sup>14</sup>

The output and transfer characteristics of BTTP-P field-effect transistors processed from chlorobenzene are shown in Figure 6. A saturation region mobility of  $1.1 \times 10^{-3}$  cm<sup>2</sup>/(V s) with an on/off current ratio of 100 was obtained (Table 1). The reason

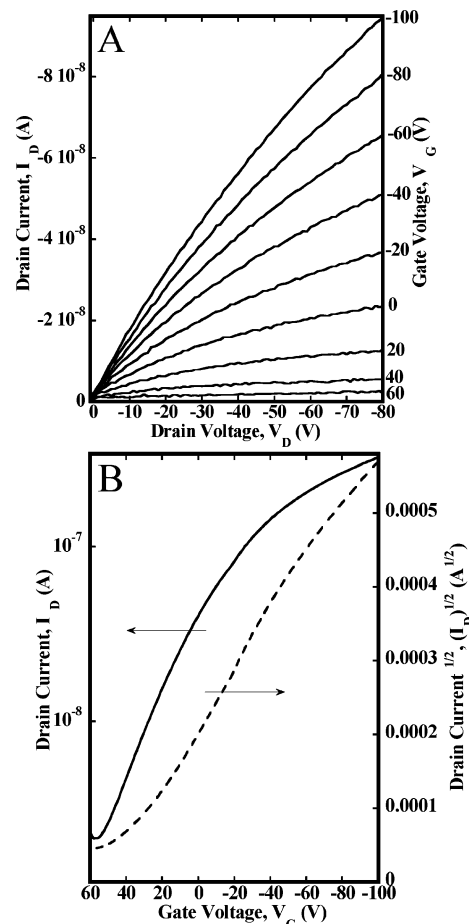


**Figure 6.** Output (A) and transfer (B) characteristics of a BTTP-P field-effect transistor (500  $\mu\text{m}$  width and 25  $\mu\text{m}$  channel length) processed from chlorobenzene.

for the observed poor on/off ratio is not yet clear; it is probably due to the low IP value (4.64 eV) and consequent unintentional oxygen doping of the BTTP-P FETs in ambient air testing. Figure 7 shows the output and transfer characteristics of BTTP-F FETs. These devices showed typical p-channel FET characteristics with good drain-current modulation and well-defined linear and saturation regions. A field-effect mobility of holes of  $9.6 \times 10^{-4}$  cm<sup>2</sup>/(V s) and an on/off ratio of  $2 \times 10^4$  were observed in BTTP-F FETs processed from chlorobenzene. A slight enhancement in hole mobility to  $1.6 \times 10^{-3}$  cm<sup>2</sup>/(V s) and similar on/off ratios were observed in BTTP-F FETs processed from the higher-boiling 1,2,4-trichlorobenzene<sup>15</sup> solutions. OFETs processed from trichlorobenzene also showed much lower threshold voltages ( $V_T = -3$  V) compared to those processed from chlorobenzene ( $V_T = -12$  V), suggesting that BTTP-F devices from 1,2,4-trichlorobenzene have more ordered polymer chains that help in minimizing structural disorder at the polymer/dielectric interface. The much lower ionization potential (5.04 eV) of BTTP-F compared to that of poly(9,9-dialkylfluorene) homopolymer (5.6–5.8 eV)<sup>12c,d</sup> facilitates hole

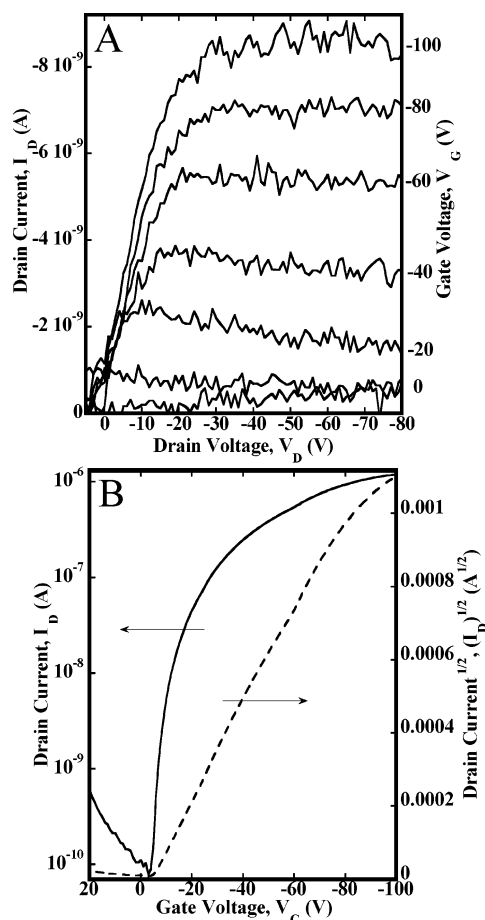


**Figure 7.** Output (A) and transfer (B) characteristics of a BTTP-F field-effect transistor (500  $\mu\text{m}$  width and 25  $\mu\text{m}$  channel length) processed from 1,2,4-trichlorobenzene.

injection and transport with respect to the gold electrodes ( $\Phi = 5.2$  eV) in the OFETs. The much higher molecular weight and thus lower concentration of chemical defects of BTTP-F ( $M_w = 172\,600$ ) than that of BTTP-P ( $M_w = 10\,000$ ) could explain its better FET performance, as found in other polymer semiconductors.<sup>6</sup>

BTTP and BTTP-T FETs processed from chlorobenzene solutions had a saturation region hole mobility of  $7.1 \times 10^{-4}$  and  $4.2 \times 10^{-4}$   $\text{cm}^2/(\text{V s})$ , respectively. However, FETs from these two copolymers had rather high “off” currents and large threshold voltages ( $>80$  V) and very low on/off current ratios. The large threshold voltages and very low on/off ratios are probably due to unintentional ambient oxygen doping of the BTTP and BTTP-T copolymer thin film FETs during the testing in air. Although the cyclic voltammetry results showed clear ambipolar redox properties, n-channel FET characteristics were not observed in any of the copolymer semiconductors. These copolymers thus did not exhibit ambipolar field-effect charge transport properties based on gold source/drain electrodes.

## Conclusions

Soluble thieno[3,4-*b*]pyrazine-based conjugated donor–acceptor polymer semiconductors with moderate to high molecular weights were synthesized by Suzuki and Stille coupling polymerizations. The strength of intramolecular charge-transfer interaction and thus the electronic and optical properties of the thieno[3,4-*b*]pyrazine-based copolymers were systematically varied by incorporating dicytlyfluorene, bis(decyloxy)phenylene, or thiophene moieties along with 5,7-bis(3-dodecylthiophen-2-

yl)thieno[3,4-*b*]pyrazine. The copolymers had small optical band gaps in the range of 1.1–1.6 eV and ambipolar redox properties with rather low ionization potentials (4.6–5.04 eV), which facilitated hole injection and transport in thin film field-effect transistors. The field-effect mobility of holes varied from  $4.2 \times 10^{-4}$   $\text{cm}^2/(\text{V s})$  for the poorly soluble BTTP-T to  $1.6 \times 10^{-3}$   $\text{cm}^2/(\text{V s})$  with an on/off ratio of  $3 \times 10^4$  in the high molecular weight BTTP-F. These results demonstrate that thieno[3,4-*b*]pyrazine-based conjugated donor–acceptor copolymers combine fairly high charge carrier mobility with broad visible-to-near-infrared absorption of interest for photovoltaic cells and other device applications.

## Experimental Section

**Materials.** All starting materials and reagents were purchased from Aldrich and used without further purification. 2-Bromo-3-dodecylthiophene,<sup>16</sup> 5,7-dibromothieno[3,4-*b*]pyrazine,<sup>17</sup> and 2,5-bis(trimethylstannyl)thiophene<sup>18</sup> were prepared according to the literature methods.

**5,7-Bis(3-dodecylthiophen-2-yl)thieno[3,4-*b*]pyrazine (1).** A Grignard reagent was prepared slowly adding a solution of 2-bromo-3-dodecylthiophene (8.38 g, 25.3 mmol) in 20 mL of anhydrous tetrahydrofuran (THF) to a stirred suspension of magnesium powder (1.1 g, 45.5 mmol) in 50 mL of THF under argon. The resulting mixture was stirred at 65  $^{\circ}\text{C}$  for 7 h. The Grignard reagent was then added via a cannula to a mixture of 5,7-dibromothieno[3,4-*b*]pyrazine (2.98 g, 10.1 mmol) and [1,3-bis(diphenylphosphino)propane]dichloronickel(II) ( $\text{NiCl}_2(\text{dppp})$ ) (137 mg, 0.25 mmol) in 100 mL of anhydrous THF at 0  $^{\circ}\text{C}$  under argon. The mixture was refluxed for 18 h. Subsequently, the reaction mixture was poured into 600 mL of water, and the product was extracted with methylene chloride ( $\text{CH}_2\text{Cl}_2$ ). The organic layer was washed twice with water and dried over anhydrous sodium sulfate. After evaporation of the solvent, the crude product was purified by column chromatography on silica gel (5% ether in hexane as eluent) to yield compound **1** as a purple solid (35%); mp 79.1–79.8  $^{\circ}\text{C}$ .  $^1\text{H}$  NMR (300 MHz,  $\text{CDCl}_3$ ):  $\delta$  8.58 (s, 2H), 7.45 (d,  $J = 5.4$  Hz, 2H), 7.08 (d,  $J = 5.1$  Hz, 2H), 2.88 (t,  $J = 7.8$  Hz, 4H), 1.71 (m,  $J = 7.2$  Hz, 4H), 1.25 (m, 36H), 0.90 (t,  $J = 6.3$  Hz, 6H). MS (ESI mode): Found  $M$ , 637.7,  $\text{C}_{38}\text{H}_{56}\text{N}_2\text{S}_3$  requires  $M$ , 637.06.

**5,7-Bis(5-bromo-3-dodecylthiophen-2-yl)thieno[3,4-*b*]pyrazine (2).** To a solution of **1** (0.76 g, 1.19 mmol) in a mixture of DMF (130 mL) and  $\text{CH}_2\text{Cl}_2$  (15 mL) at room temperature in the dark was added dropwise a solution of *N*-bromosuccinimide (0.47 g, 2.63 mmol) in DMF (20 mL). The resulting solution was stirred for 16 h and then was poured into water (500 mL). The product was extracted with  $\text{CH}_2\text{Cl}_2$ . The organic phases were washed with water and dried over sodium sulfate, and the solvent was removed under reduced pressure. The crude product was purified by column chromatography on silica gel (2% ether in hexane) to afford compound **2** (873 mg, 92%) as purple crystals; mp 81.3–81.9  $^{\circ}\text{C}$ .  $^1\text{H}$  NMR (300 MHz,  $\text{CDCl}_3$ ):  $\delta$  8.57 (s, 2H), 7.00 (s, 2H), 2.84 (t,  $J = 7.5$  Hz, 4H), 1.68 (m,  $J = 7.5$  Hz, 4H), 1.24 (m, 36H), 0.88 (t,  $J = 6.3$  Hz, 6H). MS (ESI mode): Found  $M + 1$ , 795.6,  $\text{C}_{38}\text{H}_{54}\text{Br}_2\text{N}_2\text{S}_3$  requires  $M$ , 794.85.

**2,5-Didecyloxyphenylene-1,4-bis(4,4,5,5-tetramethyl-1,3,2-dioxaborolane) (3).** *n*-BuLi (4.2 mL of 2.5 M solution in hexane, 10.5 mmol) was added dropwise to a solution of 1,4-dibromo-2,5-bis(decyloxy)benzene (2.5 g, 4.56 mmol) in THF (60 mL) at  $-78$   $^{\circ}\text{C}$  under argon. The solution was stirred at  $-78$   $^{\circ}\text{C}$  for 25 min, then warmed to 0  $^{\circ}\text{C}$ , and kept at 0  $^{\circ}\text{C}$  for 15 min. The solution was cooled to  $-78$   $^{\circ}\text{C}$  again and kept for 15 min, and 2-isopropoxy-4,4,5,5-tetramethyl-1,3,2-dioxaborolane (2.8 mL, 13.7 mmol) was added quickly. The solution was allowed to warm to room temperature and then stirred for 22 h before being poured into water. The product was extracted with ether. The organic layer was subsequently washed with water and brine and dried over sodium sulfate, and the solvent was removed by rotary evaporation. Recrystallization from a mixture of hexane/methanol afforded **3**

(50%) as white crystals; mp 76.1–77.0 °C.  $^1\text{H}$  NMR (300 MHz,  $\text{CDCl}_3$ ):  $\delta$  7.10 (s, 2H), 3.95 (t,  $J$  = 6.3 Hz, 4H), 1.77 (m,  $J$  = 6.6 Hz, 4H), 1.51 (m,  $J$  = 7.5 Hz, 4H), 1.29 (m, 48H), 0.90 (t,  $J$  = 6.9 Hz, 6H). MS (ESI mode): Found  $M + 1$ , 643.7,  $\text{C}_{38}\text{H}_{68}\text{B}_2\text{O}_6$  requires  $M$ , 642.56.

**Poly(5,7-bis(3-dodecylthiophen-2-yl)thieno[3,4-*b*]pyrazine) (BTTP).** To a mixture of **2** (300 mg, 0.38 mmol) and hexamethylditin (124 mg, 0.38 mmol) in dry chlorobenzene (8 mL) were added tris(dibenzylideneacetone)dipalladium(0) (6.9 mg, 0.007 mmol) and tri-*o*-tolylphosphine (9.2 mg, 0.03 mmol) as the catalysts. The reaction mixture was stirred at 132 °C under argon for 5 days and precipitated into a mixture of methanol (100 mL) and concentrated hydrochloric acid (5 mL) and stirred for 2 h at room temperature. The precipitate was filtered, washed with excess methanol, and dried. The polymer was purified by a Soxhlet extraction with acetone and methanol for 24 h each. After drying under vacuum, a green powder of BTTP (125 mg, 53%) was obtained.  $^1\text{H}$  NMR ( $\text{CDCl}_3$ ,  $\delta$  (ppm): 8.61 (s, 2H), 7.24 (s, 2H), 2.90 (b, 4H), 1.27 (b, 40H), 0.89 (b, 6H). FT-IR (film,  $\text{cm}^{-1}$ ): 3033, 2959, 2921, 2852, 1535, 1501, 1470, 1292, 1214, 1044, 936, 843, 723.

**Poly(5,7-bis(3-dodecylthiophen-2-yl)thieno[3,4-*b*]pyrazine-*alt*-9,9-dioctyl-2,7-fluorene) (BTTP-F).** To a three-necked flask was added 9,9-dioctylfluorene-2,7-bis(trimethyleneboronate) (281 mg, 0.5 mmol), compound **2** (400 mg, 0.5 mmol), Aliquat 336 (70 mg), and toluene (15 mL). Once the two monomers were dissolved, 2 M aqueous sodium carbonate solution (10 mL) was added. The flask equipped with a condenser was then evacuated and filled with argon several times to remove traces of air.  $\text{Pd}(\text{PPh}_3)_4$  (11.6 mg, 0.01 mmol) was then added, and the mixture was stirred for 72 h at 105 °C under argon. The reaction mixture was cooled to room temperature, and the organic layer was separated, washed with water, and precipitated into methanol. The green fibrous copolymer sample was filtered, washed with excess methanol, dried, and purified by a Soxhlet extraction with acetone for 2 days (94% yield).  $^1\text{H}$  NMR ( $\text{CDCl}_3$ ,  $\delta$  (ppm): 8.61 (s, 2H), 7.66–7.73 (m, 6H), 7.39 (s, 2H), 3.00 (b, 4H), 2.11 (b, 4H), 1.85 (b, 4H), 1.29 (b, 60H), 0.87 (b, 12H). FT-IR (film,  $\text{cm}^{-1}$ ): 3033, 2958, 2924, 2852, 1532, 1466, 1422, 1376, 1266, 1002, 935, 814, 721.

**Poly(5,7-bis(3-dodecylthiophen-2-yl)thieno[3,4-*b*]pyrazine-*alt*-1,4-bis(decyloxy)phenylene) (BTTP-P).** This copolymer was prepared by a procedure similar to that of BTTP-F using compound **3** instead of 9,9-dioctylfluorene-2,7-bis(trimethyleneboronate) as the monomer (90% yield).  $^1\text{H}$  NMR ( $\text{CDCl}_3$ ,  $\delta$  (ppm): 8.61 (s, 2H), 7.61 (s, 2H), 7.35 (s, 2H), 4.19 (m, 4H), 2.98 (m, 4H), 2.03 (m, 4H), 1.81 (m, 4H), 1.33 (b, 64H), 0.90 (b, 12H). FT-IR (film,  $\text{cm}^{-1}$ ): 3033, 2959, 2922, 2851, 1603, 1535, 1501, 1468, 1379, 1290, 1214, 1044, 936, 843, 722.

**Poly(5,7-bis(3-dodecylthiophen-2-yl)thieno[3,4-*b*]pyrazine-*alt*-2,5-thiophene) (BTTP-T).** This glossy green copolymer sample was prepared by a procedure similar to that of BTTP using 2,5-bis(trimethylstannyl)thiophene instead of hexamethylditin as the monomer (95% yield). The NMR and FT-IR spectra of this polymer were not recorded due to its poor solubility in most organic solvents.

**Characterization.** FT-IR spectra were taken on a Perkin-Elmer 1720 FTIR spectrophotometer with KBr pellets or NaCl plates.  $^1\text{H}$  NMR spectra were recorded on a Bruker-AF300 spectrometer at 300 MHz. MS spectra were obtained on a Bruker Esquire LC/ion trap mass spectrometer. Melting points were determined on an Electrothermal IA9100 digital melting point instrument at a heating rate of 1 °C/min. Gel permeation chromatography (GPC) analysis of the polymers was performed on a Waters gel permeation chromatograph with Shodex gel columns and M-150-C (64/25) detectors using trichlorobenzene as eluent and polystyrene standards as reference. Differential scanning calorimetry (DSC) analysis was performed on a TA Instruments Q100 DSC under  $\text{N}_2$  at a heating rate of 10 °C/min, and thermogravimetric analysis (TGA) analysis was conducted with a TA Instruments Q50 TGA at a heating rate of 20 °C/min under a nitrogen gas flow. UV–vis absorption spectra were recorded on a Perkin-Elmer model Lambda 900 UV/vis/near-IR spectrophotometer. The photoluminescence (PL) emission

spectra were obtained with a Photon Technology International (PTI) Inc. model QM-2001-4 spectrofluorimeter.

Cyclic voltammetry experiments were done on an EG&G Princeton Applied Research potentiostat/galvanostat (model 273A) in an electrolyte solution of 0.1 M tetrabutylammonium hexafluorophosphate ( $\text{Bu}_4\text{NPF}_6$ ) in acetonitrile. A three-electrode cell was used in all experiments. Platinum wire electrodes were used as both counter and working electrodes, and silver/silver ion (Ag in 0.1 M  $\text{AgNO}_3$  solution, Bioanalytical System, Inc.) was used as a reference electrode. The  $\text{Ag}/\text{Ag}^+$  ( $\text{AgNO}_3$ ) reference electrode was calibrated at the beginning of the experiments by running cyclic voltammetry on ferrocene as the internal standard. The potential values obtained in reference to  $\text{Ag}/\text{Ag}^+$  electrode were then converted to the saturated calomel electrode (SCE) scale. The films of the polymers were coated onto the Pt working electrode by dipping the Pt wire into a 1 wt % chlorobenzene solution of each copolymer sample and dried under vacuum at 80 °C for 24 h.

**Fabrication and Characterization of Thin Film Transistors.** Bottom-contact geometry was used to fabricate the thin-film field-effect transistors. Heavily n-doped Si with a conductivity of  $10^3$  S/cm was used as a gate electrode with 300 nm thick  $\text{SiO}_2$  layer as the gate dielectric. By use of photolithography and a vacuum sputtering system ( $2 \times 10^{-6}$  Torr), two 90 nm thick gold electrodes (source and drain) with a 10 nm thick adhesive layer of TiW alloy were fabricated onto the  $\text{SiO}_2$  layer. A channel length ( $L$ ) of 25  $\mu\text{m}$  and a channel width ( $W$ ) of 500  $\mu\text{m}$  were used. Thin films of the thienopyrazine-based D–A copolymers except BTTP-T were made by spin-coating a hot 0.2 wt % chlorobenzene or 1,2,4-trichlorobenzene solution onto modified  $\text{SiO}_2$  surface and dried for 10–12 h at 60 °C in a vacuum oven. Thin films of BTTP-T were made by drop-casting a hot 0.2 wt % chlorobenzene solution onto the FET devices. The gate electrode launching pad was placed on top of the Si gate electrode after the  $\text{SiO}_2$  gate dielectric had been mechanically etched away. Electrical characteristics of the devices were measured by using a Keithley 4200 semiconductor parameter analyzer (Keithley Instruments, Inc., Cleveland, OH). All the measurements were done under ambient laboratory conditions.

**Surface Treatment of  $\text{SiO}_2$  by Self-Assembled Monolayers (SAMs).** The  $\text{SiO}_2$  surfaces of the FET substrates were treated with octadecyltriethoxysilane (OTS-18) through a standard vapor deposition. The wafers were placed in a desiccator with a small vial of OTS-18. Then the desiccator was put under vacuum, heated to 80 °C, and left overnight for the deposition of the OTS-18 SAM on the  $\text{SiO}_2$  surface. After deposition, the FET substrates were sonicated for 1 min in anhydrous toluene and stored in vacuum before use.

**Acknowledgment.** This research was supported by the Air Force Office of Scientific Research (Grant F49620-03-1-0162), the NSF (Grant CTS-0437912), and in part by the AFOSR MURI (Grant FA9550-06-1-0326).

## References and Notes

- (a) Karikomi, M.; Kitamura, C.; Tanaka, S.; Yamashita, Y. *J. Am. Chem. Soc.* **1995**, *117*, 6791. (b) Lee, B.-L.; Yamamoto, T. *Macromolecules* **1999**, *32*, 1375. (c) Yamamoto, T.; Zhou, Z. H.; Kanbara, T.; Shimura, M.; Kizu, K.; Maruyama, T.; Nakamura, Y.; Fukuda, T.; Lee, B.-L.; Ooba, N.; Tomaru, S.; Kurihara, T.; Kaino, T.; Kubota, K.; Sasaki, S. *J. Am. Chem. Soc.* **1996**, *118*, 10389. (d) Zhang, Q. T.; Tour, J. M. *J. Am. Chem. Soc.* **1998**, *120*, 5355. (e) Jenekhe, S. A.; Lu, L.; Alam, M. M. *Macromolecules* **2001**, *34*, 7315. (f) van Mullekom, H. A. M.; Vekemans, J. A. J. M.; Havinga, E. E.; Meijer, E. W. *Mater. Sci. Eng., R* **2001**, *32*, 1.
- (a) Agrawal, A. K.; Jenekhe, S. A. *Macromolecules* **1993**, *26*, 895. (b) Agrawal, A. K.; Jenekhe, S. A. *Chem. Mater.* **1993**, *5*, 633. (c) Agrawal, A. K.; Jenekhe, S. A. *Chem. Mater.* **1996**, *8*, 579. (d) Cui, Y.; Zhang, X.; Jenekhe, S. A. *Macromolecules* **1999**, *32*, 3824. (e) Zhu, Y.; Yen, C.-T.; Jenekhe, S. A.; Chen, W.-C. *Macromol. Rapid Commun.* **2004**, *25*, 1829.
- (a) Jenekhe, S. A.; Yi, S. *Appl. Phys. Lett.* **2000**, *77*, 2635. (b) Alam, M. M.; Jenekhe, S. A. *J. Phys. Chem. B* **2001**, *105*, 2479. (c) Alam, M. M.; Jenekhe, S. A. *Chem. Mater.* **2004**, *16*, 4647. (d) Yu, G.; Gao, J.; Hummelen, J. C.; Wudl, F.; Heeger, A. J. *Science* **1995**, *270*, 1789.



- (e) Sonmez, G.; Shen, C. K. F.; Rubin, Y.; Wudl, F. *Adv. Mater.* **2005**, *17*, 897. (f) Campos, L. M.; Tontcheva, A.; Günes, S.; Sonmez, G.; Neugebauer, H.; Sariciftci, N. S.; Wudl, F. *Chem. Mater.* **2005**, *17*, 4031. (g) Svensson, M.; Zhang, F.; Veenstra, S. C.; Verhees, W. J. H.; Hummelen, J. C.; Kroon, J. M.; Inganäs, O.; Andersson, M. R. *Adv. Mater.* **2003**, *15*, 988. (h) Admassie, S.; Inganäs, O.; Mammo, W.; Perzon, E.; Andersson, M. R. *Synth. Met.* **2006**, *156*, 614.
- (4) (a) Zhang, X.; Jenekhe, S. A. *Macromolecules* **2000**, *33*, 2069. (b) Kulkarni, A. P.; Zhu, Y.; Jenekhe, S. A. *Macromolecules* **2005**, *38*, 1553. (c) Ego, C.; Marsitzky, D.; Becker, S.; Zhang, J.; Grimsdale, A. C.; Müllen, K.; MacKenzie, J. D.; Silva, C.; Friend, R. H. *J. Am. Chem. Soc.* **2003**, *125*, 437. (d) Wu, W.-C.; Liu, C.-L.; Chen, W.-C. *Polymer* **2006**, *47*, 527. (e) Thompson, B. C.; Madrigal, L. G.; Pinto, M. R.; Kang, T.-S.; Schanze, K. S.; Reynolds, J. R. *J. Polym. Sci., Part A: Polym. Chem.* **2005**, *43*, 1417. (f) Hancock, J. M.; Gifford, A. P.; Zhu, Y.; Lou, Y.; Jenekhe, S. A. *Chem. Mater.* **2006**, *18*, 4924.
- (5) (a) Champion, R. D.; Cheng, K.-F.; Pai, C.-L.; Chen, W.-C.; Jenekhe, S. A. *Macromol. Rapid Commun.* **2005**, *26*, 1835. (b) Babel, A.; Wind, J. D.; Jenekhe, S. A. *Adv. Funct. Mater.* **2004**, *14*, 891. (c) Yamamoto, T.; Yasuda, T.; Sakai, Y.; Aramaki, S. *Macromol. Rapid Commun.* **2005**, *26*, 1214. (d) Yamamoto, T.; Kokubo, H.; Kobashi, M.; Sakai, Y. *Chem. Mater.* **2004**, *16*, 4616. (e) Chen, M.; Crispin, X.; Perzon, E.; Andersson, M. R.; Pullerits, T.; Andersson, M.; Inganäs, O.; Berggren, M. *Appl. Phys. Lett.* **2005**, *87*, 252105. (f) Yasuda, T.; Sakai, Y.; Aramaki, S.; Yamamoto, T. *Chem. Mater.* **2005**, *17*, 6060.
- (6) (a) Kline, R. J.; McGehee, M. D.; Kadnikova, E. N.; Liu, J.; Fréchet, J. M. J.; Toney, M. F. *Macromolecules* **2005**, *38*, 3312. (b) Zen, A.; Saphiannikova, M.; Neher, D.; Grenzer, J.; Grigorian, S.; Pietsch, U.; Asawapirom, U.; Janietz, S.; Scherf, U.; Lieberwirth, I.; Wegner, G. *Macromolecules* **2006**, *39*, 2162.
- (7) (a) Chen, T. A.; Wu, X.; Rieke, R. D. *J. Am. Chem. Soc.* **1995**, *117*, 233. (b) Babel, A.; Jenekhe, S. A. *J. Phys. Chem. B* **2003**, *107*, 1749.
- (8) Kenning, D. D.; Rasmussen, S. C. *Macromolecules* **2003**, *36*, 6298.
- $E_{\text{red}}^{\text{onset}}$  for poly(2,3-diethylthieno[3,4-*b*]pyrazine) of  $-1.34$  V vs Ag/Ag<sup>+</sup> was reported; we converted it to  $-1.9$  V vs SCE by taking  $E$  (vs SCE) =  $E$  (vs Ag/Ag<sup>+</sup>)  $- 0.56$  V and obtained the EA to be  $-2.5$  eV by using  $EA = E_{\text{red}}^{\text{onset}} + 4.4$ .
- (9) (a) Jenekhe, S. A.; Osaheni, J. A. *Science* **1994**, *265*, 765–768. (b) Osaheni, J. A.; Jenekhe, S. A. *Macromolecules* **1994**, *27*, 739–742.
- (10) (a) Yang, C. J.; Jenekhe, S. A. *Macromolecules* **1995**, *28*, 1180. (b) Kulkarni, A. P.; Tonzola, C. J.; Babel, A.; Jenekhe, S. A. *Chem. Mater.* **2004**, *16*, 4556.
- (11) Sariciftci, N. S. *Primary Photoexcitations in Conjugated Polymers: Molecular Excitons vs Semiconductor Band Model*; World Scientific: Singapore, 1997.
- (12) (a) Babel, A.; Jenekhe, S. A. *J. Am. Chem. Soc.* **2003**, *125*, 13656. (b) Zhu, Y.; Babel, A.; Jenekhe, S. A. *Macromolecules* **2005**, *38*, 7983. (c) Babel, A.; Jenekhe, S. A. *Macromolecules* **2003**, *36*, 7759. (d) Liao, L. S.; Fung, M. K.; Lee, C. S.; Lee, S. T.; Inbasekaran, M.; Woo, E. P.; Wu, W. W. *Appl. Phys. Lett.* **2000**, *76*, 3582.
- (13) Sze, S. M. *Physics of Semiconductor Devices*; Wiley: New York, 1981.
- (14) Salleo, A.; Chabiny, M. L.; Yang, M. S.; Street, R. A. *Appl. Phys. Lett.* **2002**, *81*, 4383.
- (15) Chang, J.-F.; Sun, B.; Breiby, D. W.; Nielsen, M. M.; Sölling, T. I.; Giles, M.; McCulloch, I.; Sirringhaus, H. *Chem. Mater.* **2004**, *16*, 4772.
- (16) He, M.; Leslie, T. M.; Sinicropi, J. A. *Chem. Mater.* **2002**, *14*, 4662.
- (17) (a) Kenning, D. D.; Mitchell, K. A.; Calhoun, T. R.; Funfar, M. R.; Sattler, D. J.; Rasmussen, S. C. *J. Org. Chem.* **2002**, *67*, 9073. (b) Berlin, A.; Zotti, G.; Zecchin, S.; Schiavon, G.; Vercelli, B.; Zanelli, A. *Chem. Mater.* **2004**, *16*, 3667.
- (18) van Pham, C.; Macomber, R. S.; Mark, H. B., Jr.; Zimmer, H. J. *Org. Chem.* **1984**, *49*, 5250.

MA061861G